Multipoint Flux Approximations

Ivar Aavatsmark

Centre for Integrated Petroleum Research
University of Bergen

FVCA5, Aussois, 13 June 2008

Outline

Outline

Reservoir flow equations

Reservoir flow equations

- The equations of reservoir simulation contain variables which have elliptic and hyperbolic character.

Reservoir flow equations

- The equations of reservoir simulation contain variables which have elliptic and hyperbolic character.
- The simulations are performed on nonorthogonal rough grids.

Reservoir flow equations

- The equations of reservoir simulation contain variables which have elliptic and hyperbolic character.
- The simulations are performed on nonorthogonal rough grids.
- The medium is strongly heterogeneous.

Reservoir flow equations

- The equations of reservoir simulation contain variables which have elliptic and hyperbolic character.
- The simulations are performed on nonorthogonal rough grids.
- The medium is strongly heterogeneous.
- The permeability is often anisotropic.

Reservoir flow equations

- The equations of reservoir simulation contain variables which have elliptic and hyperbolic character.
- The simulations are performed on nonorthogonal rough grids.
- The medium is strongly heterogeneous.
- The permeability is often anisotropic.
- Here, we study control volume formulations for an elliptic model equation on quadrilateral grids.

Reservoir flow equations

- The equations of reservoir simulation contain variables which have elliptic and hyperbolic character.
- The simulations are performed on nonorthogonal rough grids.
- The medium is strongly heterogeneous.
- The permeability is often anisotropic.
- Here, we study control volume formulations for an elliptic model equation on quadrilateral grids.
- This guarantees local conservation, important for the hyperbolic part.

Outline

Model equation

Model equation

$$\begin{aligned} \operatorname{div} \boldsymbol{q} &= Q && \text{in } \Omega \\ \boldsymbol{q} &= -\boldsymbol{K} \operatorname{grad} u && \text{in } \Omega \end{aligned}$$

Model equation

$$\begin{aligned} \operatorname{div} \boldsymbol{q} &= Q && \text{in } \Omega \\ \boldsymbol{q} &= -\boldsymbol{K} \operatorname{grad} u && \text{in } \Omega \end{aligned}$$

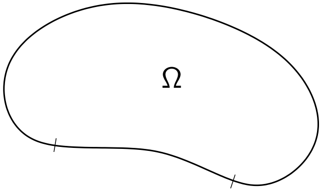

Model equation

$$\begin{aligned} \operatorname{div} \boldsymbol{q} &= Q && \text{in } \Omega \\ \boldsymbol{q} &= -\boldsymbol{K} \operatorname{grad} u && \text{in } \Omega \\ u &= u_D && \text{on } \Gamma_D \end{aligned}$$

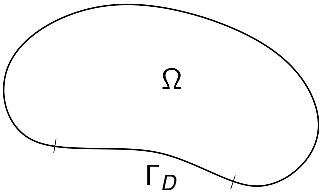

Model equation

$$\begin{aligned} \operatorname{div} \boldsymbol{q} &= Q && \text{in } \Omega \\ \boldsymbol{q} &= -\boldsymbol{K} \operatorname{grad} u && \text{in } \Omega \\ u &= u_D && \text{on } \Gamma_D \\ \boldsymbol{q} \cdot \boldsymbol{n} &= q_N && \text{on } \Gamma_N \end{aligned}$$

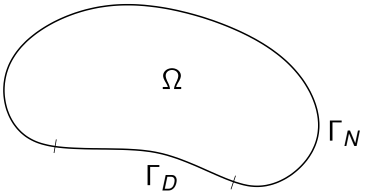

Maximum principle

Maximum principle

Suppose

$$-\operatorname{div}(\boldsymbol{K}\,\operatorname{grad} u) = q \geq 0 \quad \text{in } D.$$

Maximum principle

Suppose

$$-\operatorname{div}(\boldsymbol{K}\,\operatorname{grad} u) = q \geq 0 \quad \text{in } D.$$

Then u has no local minima in D (E. Hopf, 1927).

Maximum principle (Hopf's first lemma)

Suppose

$$-\operatorname{div}(\boldsymbol{K}\,\operatorname{grad} u) = q \geq 0 \quad \text{in } D.$$

Then u has no local minima in D (E. Hopf, 1927).

Maximum principle (Hopf's first lemma)

Suppose

$$-\operatorname{div}(\boldsymbol{K}\,\operatorname{grad} u) = q \geq 0 \quad \text{in } D.$$

Then u has no local minima in D (E. Hopf, 1927).

Green's function for homogeneous Dirichlet boundary conditions on $\Omega \subset D$: $G(\xi, \boldsymbol{x})$

Maximum principle (Hopf's first lemma)

Suppose

$$-\operatorname{div}(\boldsymbol{K} \operatorname{grad} u) = q \geq 0 \quad \text{in } D.$$

Then u has no local minima in D (E. Hopf, 1927).

Green's function for homogeneous Dirichlet boundary conditions on $\Omega \subset D$: $G(\xi, \boldsymbol{x})$

$$u(\boldsymbol{x}) = \int_\Omega G(\xi, \boldsymbol{x}) q(\xi) \, d\tau_\xi$$

Maximum principle (Hopf's first lemma)

Suppose

$$-\operatorname{div}(\boldsymbol{K}\,\operatorname{grad} u) = q \geq 0 \quad \text{in } D.$$

Then u has no local minima in D (E. Hopf, 1927).

Green's function for homogeneous Dirichlet boundary conditions on $\Omega \subset D$: $G(\xi, \boldsymbol{x})$

$$u(\boldsymbol{x}) = \int_{\Omega} G(\xi, \boldsymbol{x}) q(\xi)\, d\tau_{\xi}$$

$$G(\xi, \boldsymbol{x}) \geq 0 \qquad \xi, \boldsymbol{x} \in \Omega$$

Equivalent maximum principle

Suppose

$$-\operatorname{div}(\boldsymbol{K} \operatorname{grad} u) = q \geq 0 \quad \text{in } D.$$

Equivalent maximum principle

Suppose

$$-\operatorname{div}(\boldsymbol{K}\,\operatorname{grad} u) = q \geq 0 \quad \text{in } D.$$

Then u has no local minima in D if and only if $G(\boldsymbol{x}, \xi) \geq 0$ in Ω for all $\Omega \subset D$ with homogeneous Dirichlet boundary conditions on $\partial\Omega$.

Equivalent maximum principle

Suppose

$$-\operatorname{div}(\boldsymbol{K}\,\operatorname{grad} u) = q \geq 0 \quad \text{in } D.$$

Then u has no local minima in D if and only if $G(\boldsymbol{x}, \boldsymbol{\xi}) \geq 0$ in Ω for all $\Omega \subset D$ with homogeneous Dirichlet boundary conditions on $\partial\Omega$.

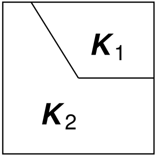

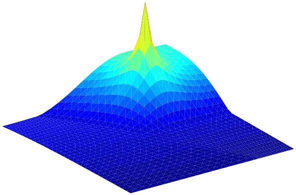

Monotonicity

Monotonicity

$G(\boldsymbol{x}, \xi) \geq 0$ implies that the operator $\mathcal{T}$, defined by

$$\mathcal{T}q = \int_{\Omega} G(\xi, \boldsymbol{x}) q \, d\tau_{\boldsymbol{\xi}},$$

is monotone in the sense that

$$q \geq 0 \quad \Rightarrow \quad \mathcal{T}q \geq 0.$$

Monotonicity

$G(\boldsymbol{x}, \xi) \geq 0$ implies that the operator $\mathcal{T}$, defined by

$$\mathcal{T}q = \int_{\Omega} G(\xi, \boldsymbol{x}) q \, d\tau_{\boldsymbol{\xi}},$$

is monotone in the sense that

$$q \geq 0 \quad \Rightarrow \quad \mathcal{T}q \geq 0.$$

We must show that $\mathcal{T}$ is monotone for all Ω with homogeneous Dirichlet boundary conditions on $\partial\Omega$.

Champagne effect

Champagne effect

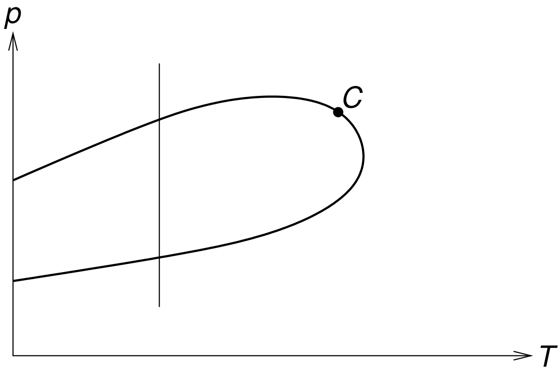

Champagne effect

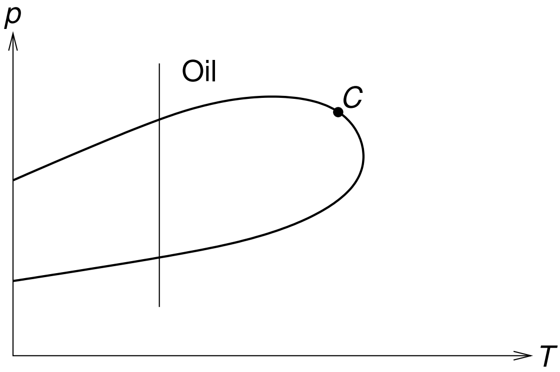

Champagne effect

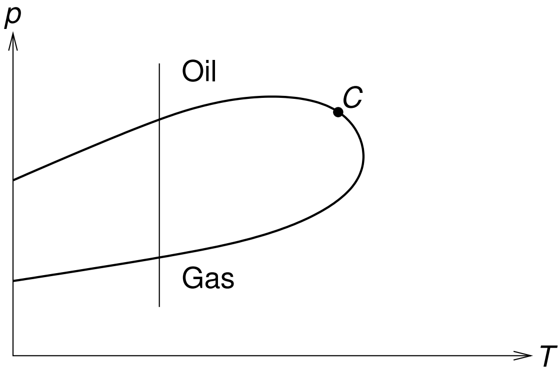

Champagne effect

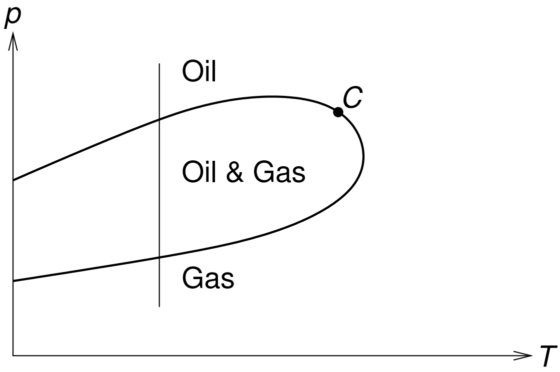

Champagne effect

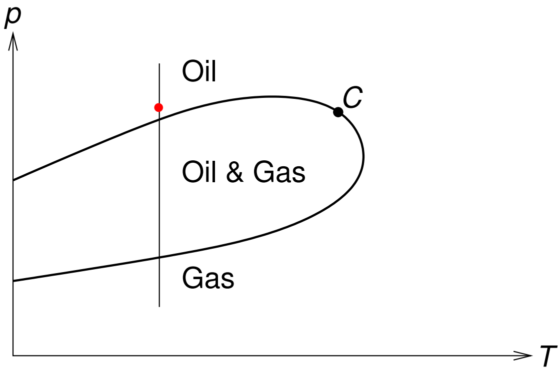

Champagne effect

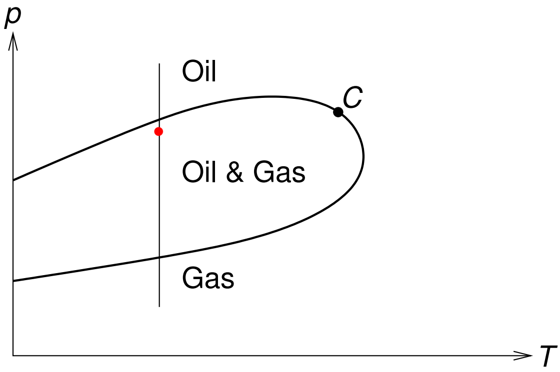

Hopf's second lemma

Hopf's second lemma

- div $\boldsymbol{q} = 0$, where $\boldsymbol{q} = -\boldsymbol{K}\,\mathrm{grad}\,u$ in Ω.

Hopf's second lemma

- div $\boldsymbol{q} = 0$, where $\boldsymbol{q} = -\boldsymbol{K}\, \text{grad}\, u$ in Ω.
- Maximum principle $\Rightarrow$ Extrema lie on the boundary.

Hopf's second lemma

- div $\boldsymbol{q} = 0$, where $\boldsymbol{q} = -\boldsymbol{K}\,\mathrm{grad}\, u$ in Ω.
- Maximum principle $\Rightarrow$ Extrema lie on the boundary.
- E. Hopf (1952): If there is an extremum on the boundary, then $\boldsymbol{q} \cdot \boldsymbol{n} \neq 0$.

Hopf's second lemma

- div $\boldsymbol{q} = 0$, where $\boldsymbol{q} = -\boldsymbol{K}\,\text{grad}\, u$ in Ω.
- Maximum principle $\Rightarrow$ Extrema lie on the boundary.
- E. Hopf (1952): If there is an extremum on the boundary, then $\boldsymbol{q} \cdot \boldsymbol{n} \neq 0$.
- Hence, extrema cannot occur on no-flow boundaries.

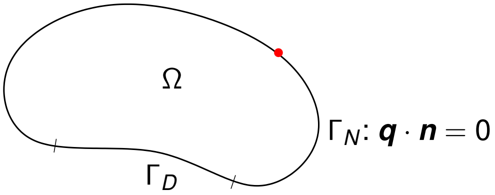

Outline

Regularity of the solution

Regularity of the solution

$$\begin{aligned} u &\in H^1(\Omega) \\ \boldsymbol{q} &\in H(\text{div}, \Omega) \end{aligned}$$

Regularity of the solution

$$u \in H^1(\Omega)$$
$$\boldsymbol{q} \in H(\mathrm{div}, \Omega)$$

- Therefore, u and $\boldsymbol{q} \cdot \boldsymbol{n}$ should have the same trace from both sides of an interface.

Regularity of the solution

$$u \in H^1(\Omega)$$
$$\boldsymbol{q} \in H(\mathrm{div}, \Omega)$$

- Therefore, u and $\boldsymbol{q} \cdot \boldsymbol{n}$ should have the same trace from both sides of an interface.
- In 1D, continuity of potential and flux yields a harmonic averaging of the permeability $\boldsymbol{K}$.

Regularity of the solution

$$u \in H^1(\Omega)$$
$$\boldsymbol{q} \in H(\text{div}, \Omega)$$

- Therefore, u and $\boldsymbol{q} \cdot \boldsymbol{n}$ should have the same trace from both sides of an interface.
- In 1D, continuity of potential and flux yields a harmonic averaging of the permeability $\boldsymbol{K}$.
- Tikhonov and Samarskij (1962) showed that harmonic averaging is crucial for maintaining the order of convergence for piecewise continuous $\boldsymbol{K}$.

Regularity of the solution

$$u \in H^1(\Omega)$$
$$\boldsymbol{q} \in H(\mathrm{div}, \Omega)$$

- Therefore, u and $\boldsymbol{q} \cdot \boldsymbol{n}$ should have the same trace from both sides of an interface.
- In 1D, continuity of potential and flux yields a harmonic averaging of the permeability $\boldsymbol{K}$.
- Tikhonov and Samarskij (1962) showed that harmonic averaging is crucial for maintaining the order of convergence for piecewise continuous $\boldsymbol{K}$.
- Method: Generalize harmonic averaging to 2D and 3D by requiring continuity in flux and (weak) continuity in potential.

Control-volume formulation

Control-volume formulation

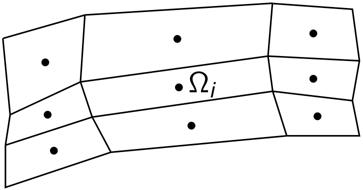

$$\int_{\partial\Omega_i} \boldsymbol{q} \cdot \boldsymbol{n} \, d\sigma = \int_{\Omega_i} Q \, d\tau$$

Control-volume formulation

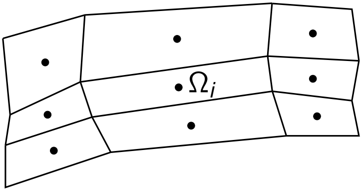

$$\int_{\partial\Omega_i} \boldsymbol{q} \cdot \boldsymbol{n} \, d\sigma = \int_{\Omega_i} Q \, d\tau$$

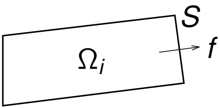

$$f = \int_S \boldsymbol{q} \cdot \boldsymbol{n} \, d\sigma$$

O-method

O-method

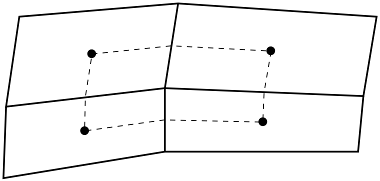

Cells with common corner

O-method

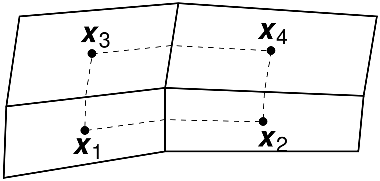

Cells with common corner

O-method

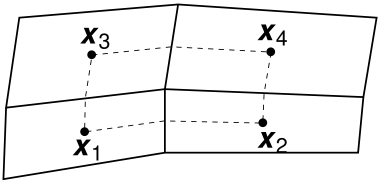

Cells with common corner

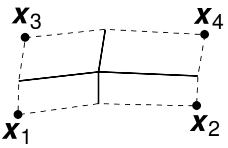

Interaction volume

O-method

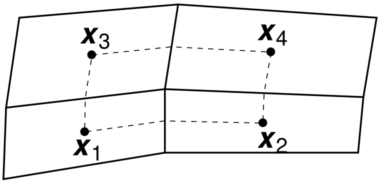

Cells with common corner

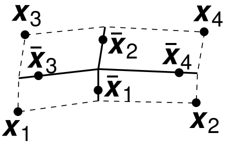

Interaction volume

O-method

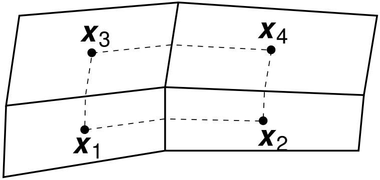

Cells with common corner

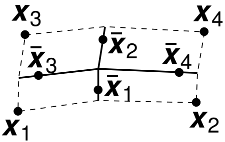

Interaction volume

- Determine the flux through the half edges from the interaction of linear potentials in the four cells.

O-method

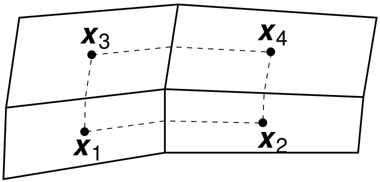

Cells with common corner

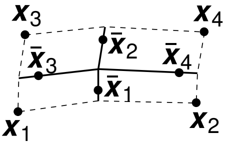

Interaction volume

- Determine the flux through the half edges from the interaction of linear potentials in the four cells.
- Require continuous potential at $\bar{\boldsymbol{x}}_i$ and continuous flux through the half edges.

Flux equations in an interaction region

Flux equations in an interaction region

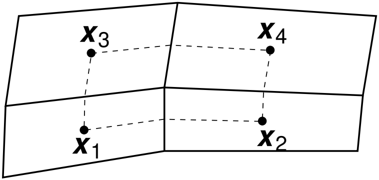

Cells with common corner

Flux equations in an interaction region

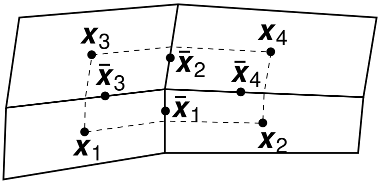

Cells with common corner

Flux equations in an interaction region

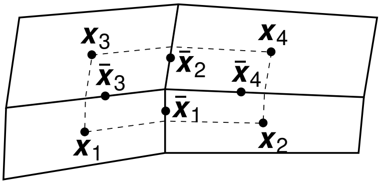

Cells with common corner

$$f_1 = f_1^{(1)} = f_1^{(2)}$$
$$f_2 = f_2^{(4)} = f_2^{(3)}$$
$$f_3 = f_3^{(3)} = f_3^{(1)}$$
$$f_4 = f_4^{(2)} = f_4^{(4)}$$

Flux equations in an interaction region

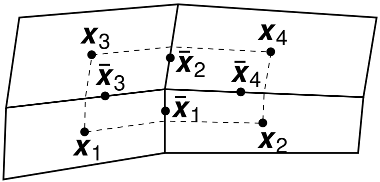

Cells with common corner

$$f_1 = f_1^{(1)} = f_1^{(2)}$$
$$f_2 = f_2^{(4)} = f_2^{(3)}$$
$$f_3 = f_3^{(3)} = f_3^{(1)}$$
$$f_4 = f_4^{(2)} = f_4^{(4)}$$

$\Rightarrow$ Local explicit expression for the half-edge fluxes

Flux expression

Flux expression

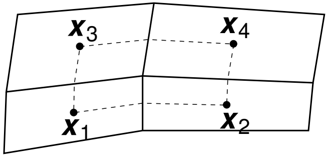

Cells with common corner

$$f_i = \sum_{j=1}^{4} t_{i,j} u_j \quad \text{where} \quad \sum_{j=1}^{4} t_{i,j} = 0$$

Flux expression

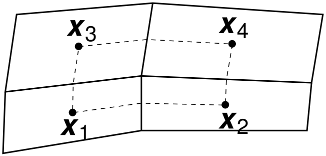

Cells with common corner

$$f_i = \sum_{j=1}^{4} t_{i,j} u_j \quad \text{where} \quad \sum_{j=1}^{4} t_{i,j} = 0$$

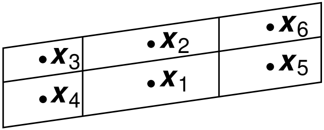

Flux stencil

$$f_i = \sum_{j=1}^{6} t_{i,j} u_j \quad \text{where} \quad \sum_{j=1}^{6} t_{i,j} = 0$$

Flux expression

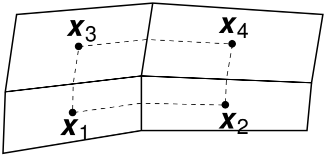

Cells with common corner

$$f_i = \sum_{j=1}^{4} t_{i,j} u_j \quad \text{where} \quad \sum_{j=1}^{4} t_{i,j} = 0$$

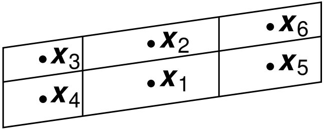

Flux stencil

$$f_i = \sum_{j=1}^{6} t_{i,j} u_j \quad \text{where} \quad \sum_{j=1}^{6} t_{i,j} = 0$$

Multipoint flux approximation (MPFA)

Stencils

Stencils

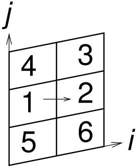

i-flux stencil

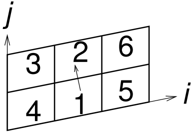

j-flux stencil

Stencils

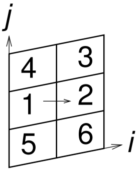

i-flux stencil

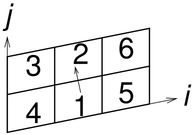

j-flux stencil

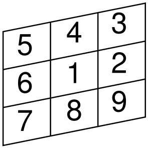

Cell stencil

O(η)-methods, Edwards et al., 1998

O(η)-methods, Edwards et al., 1998

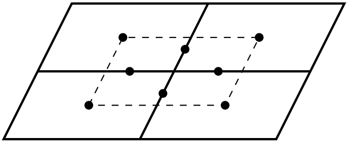

O(η)-method

O(η)-methods, Edwards et al., 1998

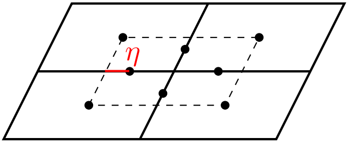

O(η)-method

Polygonal and triangular grids

Polygonal and triangular grids

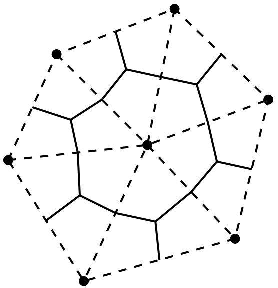

Cell stencil in polygonal grid

Polygonal and triangular grids

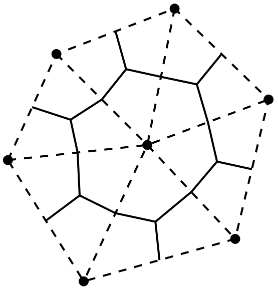

Cell stencil in polygonal grid

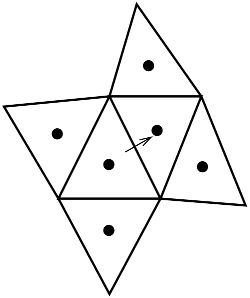

Flux stencil in triangular grid

MPFA O-method

MPFA O-method

- For non-parallelogram quadrilaterals with strong irregularity, convergence may be lost, Klausen et al. (2006).

MPFA O-method

- For non-parallelogram quadrilaterals with strong irregularity, convergence may be lost, Klausen et al. (2006).
- For high skewness combined with strong aspect or anisotropy ratio, oscillating solutions may occur.

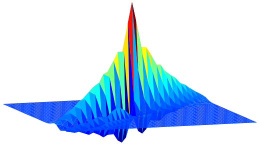

Anisotropy ratio 1 : 1000
$\theta = 30^\circ$
Square grid

Challenges

Challenges

- Are there MPFA-methods with a larger domain of validity for convergence and monotonicity?

Challenges

- Are there MPFA-methods with a larger domain of validity for convergence and monotonicity?
- Are there methods which behave less oscillatory when monotonicity cannot be assured?

Challenges

- Are there MPFA-methods with a larger domain of validity for convergence and monotonicity?
- Are there methods which behave less oscillatory when monotonicity cannot be assured?
- Does such a new method have disadvantages?

Outline

L-method

L-method

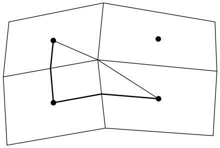

L-shaped coupling

L-method

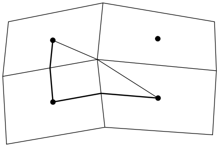

L-shaped coupling

Inside the “triangle”:

L-method

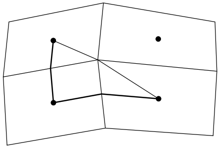

L-shaped coupling

Inside the “triangle”:

- Linear potential in each cell

L-method

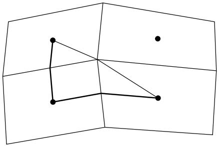

L-shaped coupling

Inside the “triangle”:

- Linear potential in each cell
- Full potential continuity

L-method

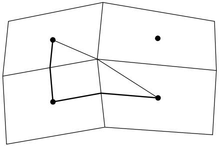

L-shaped coupling

Inside the “triangle”:

- Linear potential in each cell
- Full potential continuity
- Flux continuity

L-method

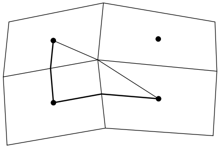

L-shaped coupling

Inside the "triangle":

- Linear potential in each cell
- Full potential continuity
- Flux continuity
- $3 \cdot 2 = 6$ deg. of freedom

L-method

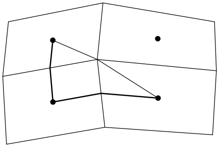

L-shaped coupling

Inside the "triangle":

- Linear potential in each cell
- Full potential continuity
- Flux continuity
- $3 \cdot 2 = 6$ deg. of freedom
- $2 \cdot 3 = 6$ conditions

Interaction region

Interaction region

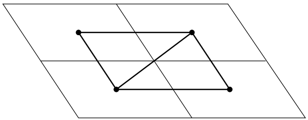

Interaction region

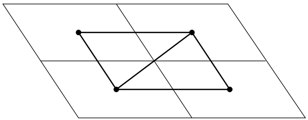

Short diagonal

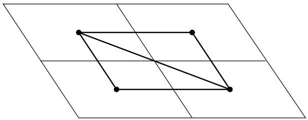

Long diagonal

7-point cell stencil

7-point cell stencil

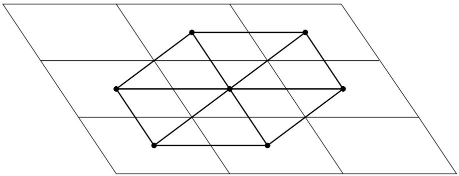

Cell stencil

7-point cell stencil

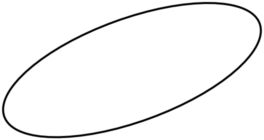

Permeability ellipse

$\boldsymbol{x}^{\mathrm{T}}\boldsymbol{K}^{-1}\boldsymbol{x} = 1$

7-point cell stencil

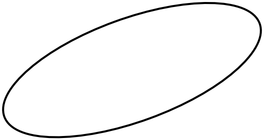

Permeability ellipse
$\boldsymbol{x}^{\mathrm{T}}\boldsymbol{K}^{-1}\boldsymbol{x} = 1$

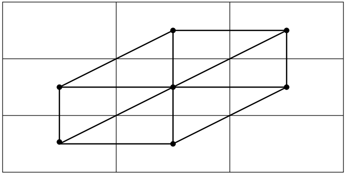

Cell stencil

General case

General case

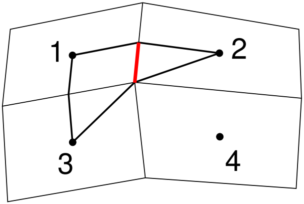

Triangle 1
Transmissibilities: t_j^1

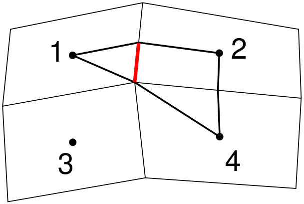

Triangle 2
Transmissibilities: t_j^2

General case

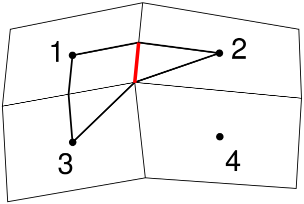

Triangle 1
Transmissibilities: t_j^1

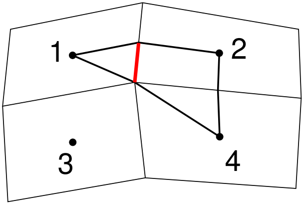

Triangle 2
Transmissibilities: t_j^2

If $|t_1^1| < |t_2^2|$, triangle 1 is chosen, else triangle 2 is chosen.

Top edge

Top edge

+	−
+	

+	−
	+

Top edge

+	−
+	

+	−
	+

- For moderate skewness, the choice will be between these cases, and it is natural to choose the case to the left.

Top edge

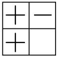

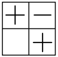

- For moderate skewness, the choice will be between these cases, and it is natural to choose the case to the left.
- For homogeneous medium and uniform grid, the criterion always chooses the “natural” seven-point stencil.

Top edge

+	−
+	

+	−
	+

- For moderate skewness, the choice will be between these cases, and it is natural to choose the case to the left.
- For homogeneous medium and uniform grid, the criterion always chooses the "natural" seven-point stencil.

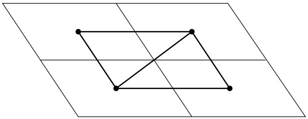

Top edge

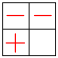

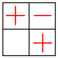

- For moderate skewness, the choice will be between these cases, and it is natural to choose the case to the left.
- For homogeneous medium and uniform grid, the criterion always chooses the “natural” seven-point stencil.

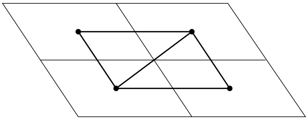

Enriched MPFA method [Chen et al., 2008]

Enriched MPFA method [Chen et al., 2008]

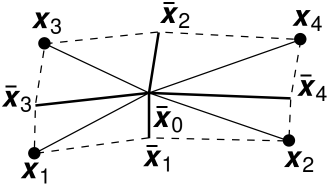

E1

Enriched MPFA method [Chen et al., 2008]

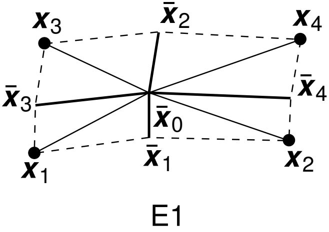

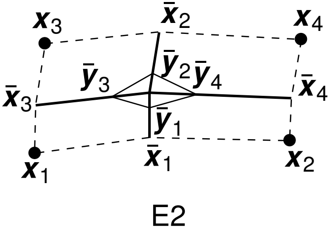

$$\lim_{\epsilon \to 0} \frac{1}{\epsilon} \int_{\bar{\boldsymbol{y}}_1 \bar{\boldsymbol{y}}_2 \bar{\boldsymbol{y}}_3 \bar{\boldsymbol{y}}_4} \boldsymbol{n} \cdot \boldsymbol{q} \, ds = 0$$

Outline

Discrete monotonicity

Discrete monotonicity

Solution of differential equation with homogeneous Dirichlet boundary conditions

$$u = \mathcal{T} q,$$

where the operator $\mathcal{T}$ is a monotone operator.

Discrete monotonicity

Solution of differential equation with homogeneous Dirichlet boundary conditions

$$u = \mathcal{T} q,$$

where the operator $\mathcal{T}$ is a monotone operator.
Associated discrete system

$$\boldsymbol{A}\boldsymbol{u} = \boldsymbol{q}.$$

Discrete monotonicity

Solution of differential equation with homogeneous Dirichlet boundary conditions

$$u = \mathcal{T} q,$$

where the operator $\mathcal{T}$ is a monotone operator.
Associated discrete system

$$\boldsymbol{A}\boldsymbol{u} = \boldsymbol{q}.$$

The matrix $\boldsymbol{A}^{-1}$ is monotone if

$$\boldsymbol{A}^{-1} \geq \boldsymbol{O}.$$

Discrete monotonicity

Solution of differential equation with homogeneous Dirichlet boundary conditions

$$u = \mathcal{T} q,$$

where the operator $\mathcal{T}$ is a monotone operator.
Associated discrete system

$$\boldsymbol{A}\boldsymbol{u} = \boldsymbol{q}.$$

The matrix $\boldsymbol{A}^{-1}$ is monotone if

$$\boldsymbol{A}^{-1} \geq \boldsymbol{O}.$$

Then

$$\boldsymbol{q} \geq \boldsymbol{0} \quad \Rightarrow \quad \boldsymbol{u} \geq \boldsymbol{0}.$$

Discrete maximum principle

Discrete maximum principle

Natural discrete analogue of the maximum principle:

$$\boldsymbol{A}^{-1} \geq \boldsymbol{O}$$

for all subgrids with homogeneous Dirichlet boundary conditions.

Discrete maximum principle

Natural discrete analogue of the maximum principle:

$$\boldsymbol{A}^{-1} \geq \boldsymbol{O}$$

for all subgrids with homogeneous Dirichlet boundary conditions.
The associated scheme is then called monotone.

Discrete maximum principle

Natural discrete analogue of the maximum principle:

$$\boldsymbol{A}^{-1} \geq \boldsymbol{O}$$

for all subgrids with homogeneous Dirichlet boundary conditions.
The associated scheme is then called monotone.

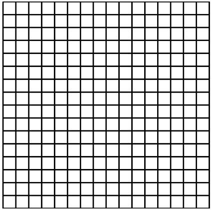

Discrete maximum principle

Natural discrete analogue of the maximum principle:

$$\boldsymbol{A}^{-1} \geq \boldsymbol{O}$$

for all subgrids with homogeneous Dirichlet boundary conditions.
The associated scheme is then called monotone.

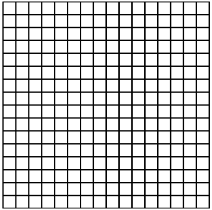

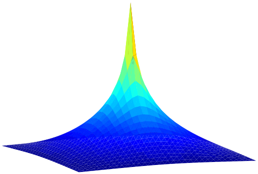

$$\boldsymbol{A}^{-1} \geq \boldsymbol{O}$$

Nonmonotone examples

Nonmonotone examples

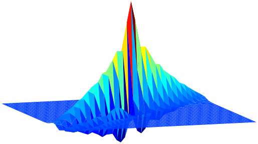

Anisotropy ratio 1 : 1000

$\theta = \pi/6$

$\eta = 0$

$\boldsymbol{A}^{-1} \not\geq \boldsymbol{O}$

Nonmonotone examples

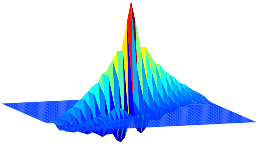

Anisotropy ratio 1 : 1000

$\theta = \pi/6$

$\eta = 0$

$\boldsymbol{A}^{-1} \ngeq \boldsymbol{O}$

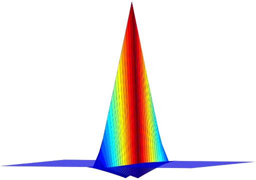

Anisotropy ratio 1 : 10000

$\theta = 0$

$\eta = 0.5$

$\boldsymbol{A}^{-1} \ngeq \boldsymbol{O}$

Outline

Monotone matrices

Monotone matrices

Conditions for $\boldsymbol{A}^{-1} \geq \boldsymbol{O}$

Monotone matrices

Conditions for $\boldsymbol{A}^{-1} \geq \boldsymbol{O}$

- For which matrices $\boldsymbol{A}$ does this hold?

Monotone matrices

Conditions for $\boldsymbol{A}^{-1} \geq \boldsymbol{O}$

- For which matrices $\boldsymbol{A}$ does this hold?
- For which stencils does this hold?

Monotone matrices

Conditions for $\boldsymbol{A}^{-1} \geq \boldsymbol{O}$

- For which matrices $\boldsymbol{A}$ does this hold?
- For which stencils does this hold?

$$-\int_{\Omega_{i,j}} \operatorname{div}(\boldsymbol{K} \operatorname{grad} u)\, d\tau \approx \sum_{k=1}^{9} m_k^{i,j} u_k$$

Monotone matrices

Conditions for $\boldsymbol{A}^{-1} \geq \boldsymbol{O}$

- For which matrices $\boldsymbol{A}$ does this hold?
- For which stencils does this hold?

$$-\int_{\Omega_{i,j}} \mathrm{div}(\boldsymbol{K}\,\mathrm{grad}\,u)\,d\tau \approx \sum_{k=1}^{9} m_k^{i,j} u_k$$

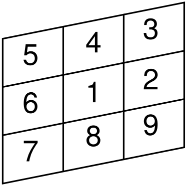

Splittings

Splittings

- The matrix $\boldsymbol{A}$ is splitted into two matrices $\boldsymbol{A} = \boldsymbol{B} - \boldsymbol{C}$.

Splittings

- The matrix $\boldsymbol{A}$ is splitted into two matrices $\boldsymbol{A} = \boldsymbol{B} - \boldsymbol{C}$.
- If

$$\boldsymbol{B}^{-1} \geq \boldsymbol{O},$$
$$\boldsymbol{B}^{-1}\boldsymbol{C} \geq \boldsymbol{O},$$

then the splitting $\boldsymbol{A} = \boldsymbol{B} - \boldsymbol{C}$ is weakly regular.

Splittings

- The matrix $\boldsymbol{A}$ is splitted into two matrices $\boldsymbol{A} = \boldsymbol{B} - \boldsymbol{C}$.
- If

$$\begin{aligned} \boldsymbol{B}^{-1} &\geq \boldsymbol{O}, \\ \boldsymbol{B}^{-1}\boldsymbol{C} &\geq \boldsymbol{O}, \end{aligned}$$

then the splitting $\boldsymbol{A} = \boldsymbol{B} - \boldsymbol{C}$ is weakly regular. It follows:

$$\boldsymbol{A}^{-1} \geq \boldsymbol{O} \qquad \Leftrightarrow \qquad \rho(\boldsymbol{B}^{-1}\boldsymbol{C}) < 1$$

Splittings

Splittings

- Suppose $\boldsymbol{A}$ has a weakly regular splitting $\boldsymbol{A} = \boldsymbol{B} - \boldsymbol{C}$.

Splittings

- Suppose $\boldsymbol{A}$ has a weakly regular splitting $\boldsymbol{A} = \boldsymbol{B} - \boldsymbol{C}$.
- If

$$\boldsymbol{A}\boldsymbol{e} \geq \mathbf{0},$$
$$\boldsymbol{B}^{-1}\boldsymbol{C} \text{ irreducible},$$

then $\rho(\boldsymbol{B}^{-1}\boldsymbol{C}) < 1$.

Splittings

- Suppose $\boldsymbol{A}$ has a weakly regular splitting $\boldsymbol{A} = \boldsymbol{B} - \boldsymbol{C}$.
- If

$$\boldsymbol{A}\boldsymbol{e} \geq \boldsymbol{0},$$
$$\boldsymbol{B}^{-1}\boldsymbol{C} \text{ irreducible},$$

  then $\rho(\boldsymbol{B}^{-1}\boldsymbol{C}) < 1$.
- Generalization of M-matrix theory.

Splittings

Splittings

- Splitting $\boldsymbol{A} = \boldsymbol{B} - \boldsymbol{C}$.

Splittings

- Splitting $\boldsymbol{A} = \boldsymbol{B} - \boldsymbol{C}$.
- If

$$\begin{aligned} \boldsymbol{e}^{\mathrm{T}}\boldsymbol{A} &\geq \mathbf{0}^{\mathrm{T}}, \\ \boldsymbol{B}^{-1} &\geq \boldsymbol{O}, \\ \boldsymbol{C}\boldsymbol{B}^{-1} &\geq \boldsymbol{O}, \\ \boldsymbol{C}\boldsymbol{B}^{-1} &\text{ irreducible,} \end{aligned}$$

then $\boldsymbol{A}^{-1} \geq \boldsymbol{O}$.

Splittings

- Splitting $\boldsymbol{A} = \boldsymbol{B} - \boldsymbol{C}$.
- If

$$\begin{aligned} \boldsymbol{e}^{\mathrm{T}}\boldsymbol{A} &\geq \boldsymbol{0}^{\mathrm{T}}, \\ \boldsymbol{B}^{-1} &\geq \boldsymbol{O}, \\ \boldsymbol{C}\boldsymbol{B}^{-1} &\geq \boldsymbol{O}, \\ \boldsymbol{C}\boldsymbol{B}^{-1} &\text{ irreducible}, \end{aligned}$$

  then $\boldsymbol{A}^{-1} \geq \boldsymbol{O}$.
- These conditions are only sufficient.

Monotonicity criteria

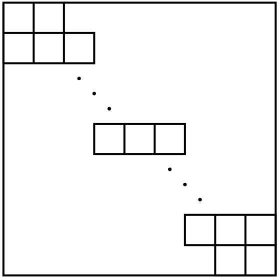

A block-tridiagonal

Monotonicity criteria

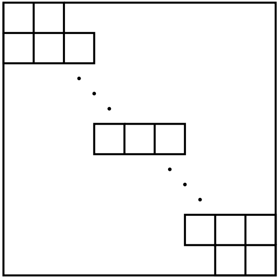

$\boldsymbol{A}$ block-tridiagonal

- $\boldsymbol{A} = \boldsymbol{B} - \boldsymbol{C}$,

Monotonicity criteria

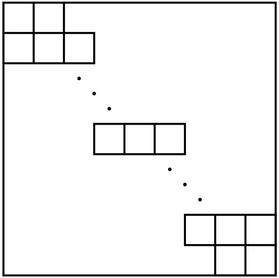

$\boldsymbol{A}$ block-tridiagonal

- $\boldsymbol{A} = \boldsymbol{B} - \boldsymbol{C}$,
- $\boldsymbol{B} =$ diagonal blocks,

Monotonicity criteria

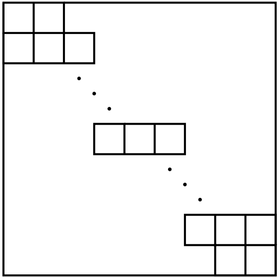

$\boldsymbol{A}$ block-tridiagonal

- $\boldsymbol{A} = \boldsymbol{B} - \boldsymbol{C}$,
- $\boldsymbol{B}$ = diagonal blocks,
- $-\boldsymbol{C}$ = offdiagonal blocks,

Monotonicity criteria

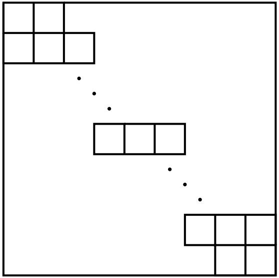

$\boldsymbol{A}$ block-tridiagonal

- $\boldsymbol{A} = \boldsymbol{B} - \boldsymbol{C}$,
- $\boldsymbol{B} =$ diagonal blocks,
- $-\boldsymbol{C} =$ offdiagonal blocks,
- Different orderings yield different conditions.

Monotonicity criteria

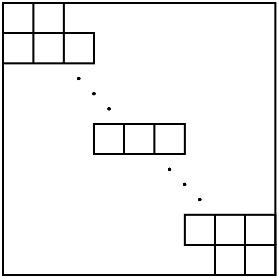

$\boldsymbol{A}$ block-tridiagonal

- $\boldsymbol{A} = \boldsymbol{B} - \boldsymbol{C}$,
- $\boldsymbol{B} =$ diagonal blocks,
- $-\boldsymbol{C} =$ offdiagonal blocks,
- Different orderings yield different conditions.
- Use rowwise or columnwise orderings.

Rowwise ordering

$$\begin{aligned}
m_1^{i,j} &> 0\\
m_2^{i,j} &< 0\\
m_6^{i,j} &< 0\\
m_4^{i,j} &< 0\\
m_8^{i,j} &< 0\\
m_1^{i,j} + m_2^{i,j} + m_6^{i,j} &> 0\\
m_2^{i,j} m_4^{i,j-1} - m_3^{i,j-1} m_1^{i,j} &> 0\\
m_6^{i,j} m_4^{i,j-1} - m_5^{i,j-1} m_1^{i,j} &> 0\\
m_2^{i,j} m_8^{i,j+1} - m_9^{i,j+1} m_1^{i,j} &> 0\\
m_6^{i,j} m_8^{i,j+1} - m_7^{i,j+1} m_1^{i,j} &> 0
\end{aligned}$$

Columnwise ordering

$$
\begin{aligned}
m_1^{i,j} &> 0 \\
m_2^{i,j} &< 0 \\
m_4^{i,j} &< 0 \\
m_6^{i,j} &< 0 \\
m_8^{i,j} &< 0 \\
m_1^{i,j} + m_4^{i,j} + m_8^{i,j} &> 0 \\
m_4^{i,j} m_2^{i-1,j} - m_3^{i-1,j} m_1^{i,j} &> 0 \\
m_4^{i,j} m_6^{i+1,j} - m_5^{i+1,j} m_1^{i,j} &> 0 \\
m_8^{i,j} m_2^{i-1,j} - m_9^{i-1,j} m_1^{i,j} &> 0 \\
m_8^{i,j} m_6^{i+1,j} - m_7^{i+1,j} m_1^{i,j} &> 0
\end{aligned}
$$

Local monotonicity criteria

Local monotonicity criteria

- Different orderings yield different criteria.

Local monotonicity criteria

- Different orderings yield different criteria.
- Local, explicit criteria apply for each grid cell.

Local monotonicity criteria

- Different orderings yield different criteria.
- Local, explicit criteria apply for each grid cell.
- Criteria apply to general cases of heterogeneity and geometry.

Local monotonicity criteria

- Different orderings yield different criteria.
- Local, explicit criteria apply for each grid cell.
- Criteria apply to general cases of heterogeneity and geometry.
- Agreement with numerical observations.

Homogeneous medium, uniform grid

Homogeneous medium, uniform grid

$$\begin{aligned} m_1 &> 0 \\ \max\{m_2, m_4\} &< 0 \\ m_1 + 2\max\{m_2, m_4\} &> 0 \\ m_2 m_4 - \max\{m_3, m_5\} \cdot m_1 &> 0 \end{aligned}$$

Homogeneous medium, uniform grid

$$\begin{aligned} m_1 &> 0 \\ \max\{m_2, m_4\} &< 0 \\ m_1 + 2\max\{m_2, m_4\} &> 0 \\ m_2 m_4 - \max\{m_3, m_5\} \cdot m_1 &> 0 \end{aligned}$$

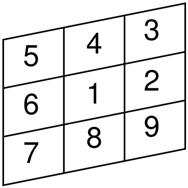

Monotonicity

Monotonicity

Homogeneous medium
Uniform grid

Monotonicity

Homogeneous medium
Uniform grid

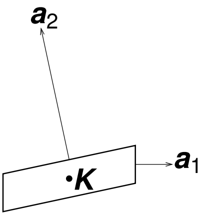

Monotonicity

Homogeneous medium
Uniform grid

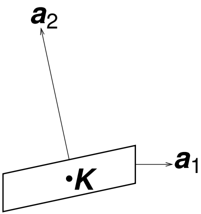

Define

$$\begin{bmatrix} a & c \\ c & b \end{bmatrix} = \frac{1}{V} \begin{bmatrix} \boldsymbol{a}_1 & \boldsymbol{a}_2 \end{bmatrix}^{\mathrm{T}} \boldsymbol{K} \begin{bmatrix} \boldsymbol{a}_1 & \boldsymbol{a}_2 \end{bmatrix}$$

Monotonicity

Homogeneous medium
Uniform grid

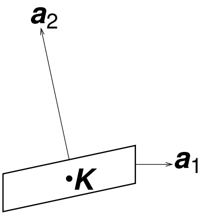

Define

$$\begin{bmatrix} a & c \\ c & b \end{bmatrix} = \frac{1}{V} \begin{bmatrix} \boldsymbol{a}_1 & \boldsymbol{a}_2 \end{bmatrix}^{\mathrm{T}} \boldsymbol{K} \begin{bmatrix} \boldsymbol{a}_1 & \boldsymbol{a}_2 \end{bmatrix}$$

Ellipticity implies

$$c \leq \sqrt{ab}$$

Monotonicity

Homogeneous medium
Uniform grid

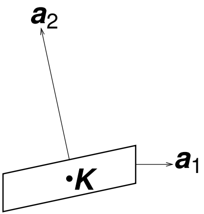

Define

$$\begin{bmatrix} a & c \\ c & b \end{bmatrix} = \frac{1}{V} \begin{bmatrix} \boldsymbol{a}_1 & \boldsymbol{a}_2 \end{bmatrix}^{\mathrm{T}} \boldsymbol{K} \begin{bmatrix} \boldsymbol{a}_1 & \boldsymbol{a}_2 \end{bmatrix}$$

Ellipticity implies

$$c \leq \sqrt{ab}$$

Monotonicity & conservation & exact solution for uniform flow imply

$$c \leq \min\{a, b\}.$$

Monotonicity

Monotonicity

Assume $a \leq b$

Monotonicity

Assume $a \leq b$

Ellipticity:

$$\frac{c}{b} \leq \sqrt{\frac{a}{b}}$$

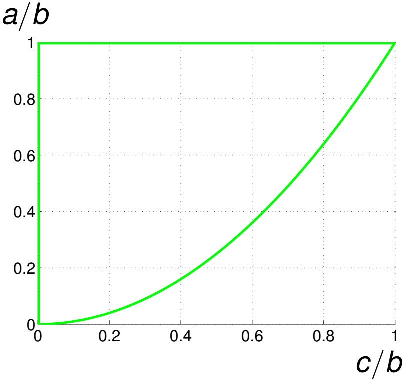

Monotonicity

Assume $a \leq b$

Ellipticity:

$$\frac{c}{b} \leq \sqrt{\frac{a}{b}}$$

Monotonicity:

$$\frac{c}{b} \leq \frac{a}{b}$$

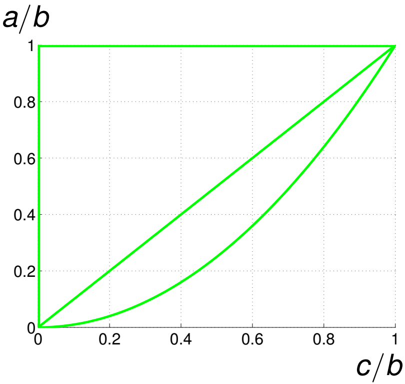

Monotonicity, $\eta = 0$

Assume $a \leq b$

Ellipticity:

$$\frac{c}{b} \leq \sqrt{\frac{a}{b}}$$

Monotonicity:

$$\frac{c}{b} \leq \frac{a}{b}$$

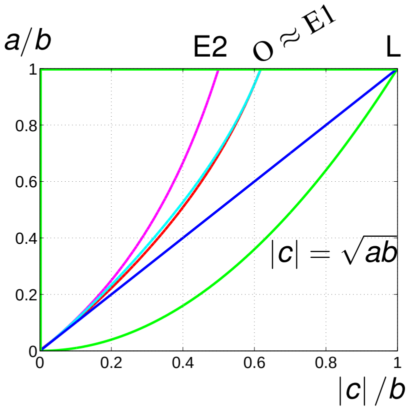

Monotonicity, $\eta = 0$

Assume $a \leq b$

Ellipticity:

$$\frac{c}{b} \leq \sqrt{\frac{a}{b}}$$

Monotonicity:

$$\frac{c}{b} \leq \frac{a}{b}$$

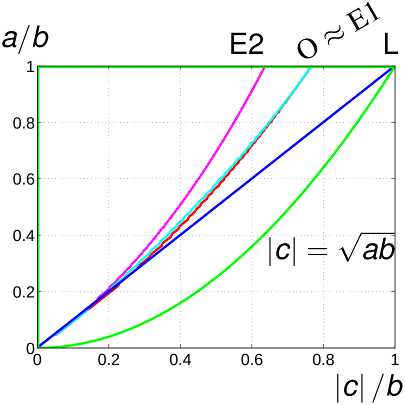

Monotonicity, $\eta = 0.5$

Assume $a \leq b$

Ellipticity:

$$\frac{c}{b} \leq \sqrt{\frac{a}{b}}$$

Monotonicity:

$$\frac{c}{b} \leq \frac{a}{b}$$

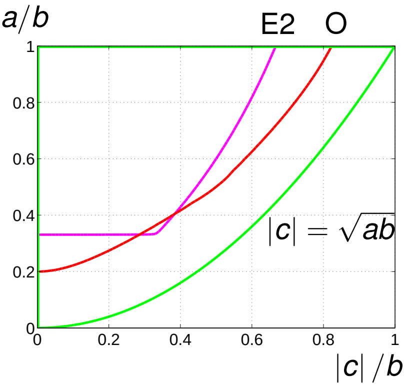

Monotonicity, $\eta = 0$

Assume $a \le b$

Ellipticity:

$$\frac{c}{b} \le \sqrt{\frac{a}{b}}$$

Monotonicity:

$$\frac{c}{b} \le \frac{a}{b}$$

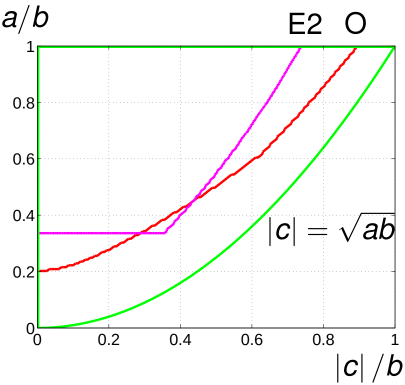

Layered media and uniform grids. O(0)-method.

Layered media and uniform grids. O(0)-method.

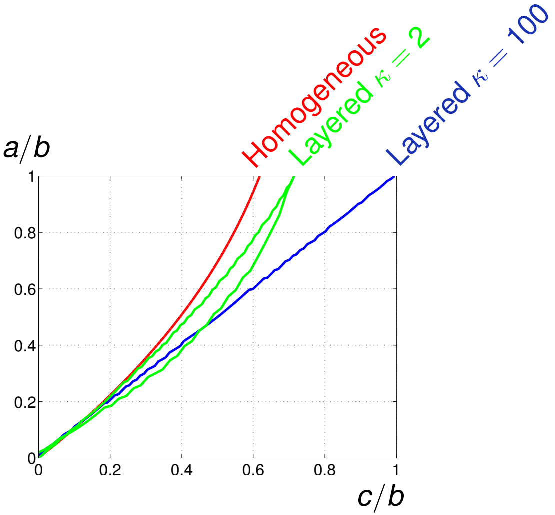

Layered media and uniform grids. O(0)-method.

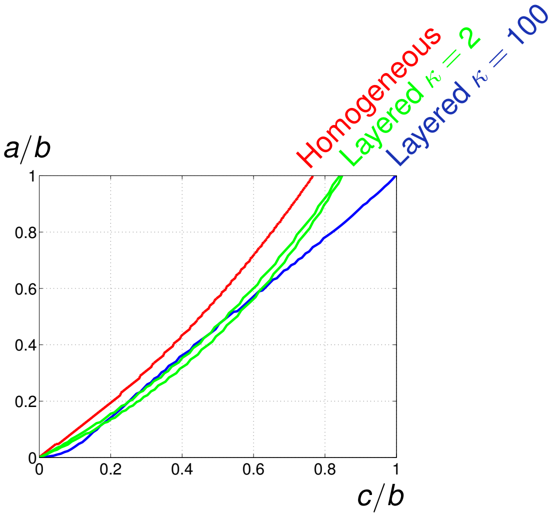

Outline

Nonmonotone case

Nonmonotone case

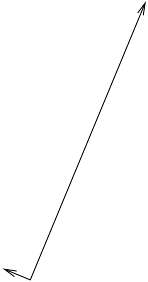

Anisotropy 1:1000

Angle 67.5 $^\circ$

Square grid cells

Nonmonotone case

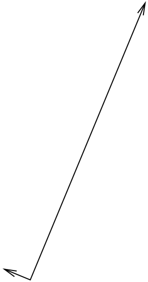

Anisotropy 1:1000
Angle 67.5 $^\circ$
Square grid cells

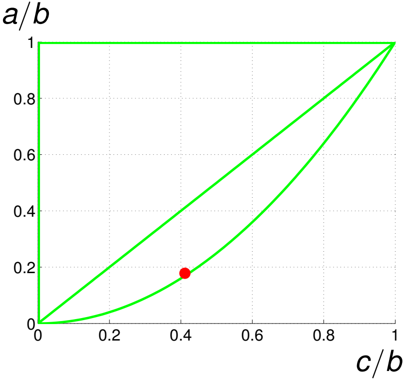

$a/b = 0.41$
$c/b = 0.17$

19×3 grid, single source in cell $(10, 3)$

19×3 grid, single source in cell $(10, 3)$

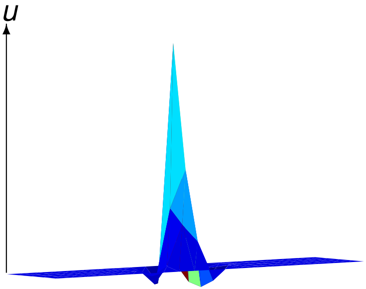

L-method

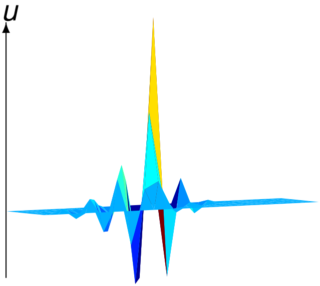

O-method

19 $\times$ 3 grid, single source in cell $(10, 3)$

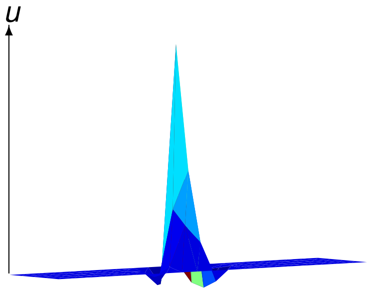

L-method

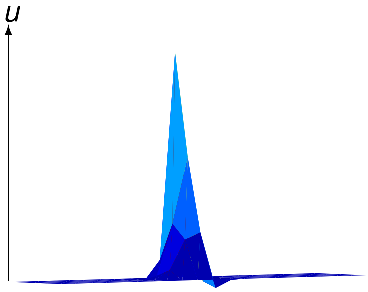

E1-method

19×3 grid, single source in cell $(10, 3)$

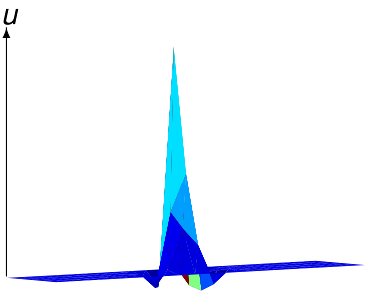

L-method

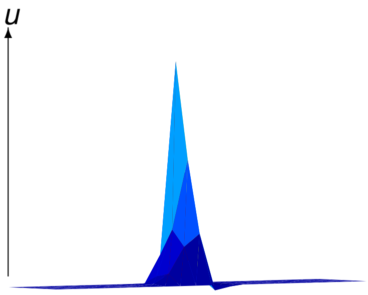

E2-method

19×3 grid, single source in cell $(10, 3)$

19×3 grid, single source in cell $(10, 3)$

Oscillating behavior (violation of Hopf 1):

19×3 grid, single source in cell $(10, 3)$

Oscillating behavior (violation of Hopf 1):

- L, E1, E2 much better than O,

19×3 grid, single source in cell $(10, 3)$

Oscillating behavior (violation of Hopf 1):

- L, E1, E2 much better than O,
- E2 and E1 marginally better than L.

A case with no-flow boundary

A case with no-flow boundary

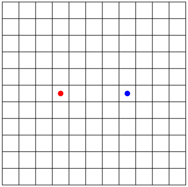

- pressure 0
- pressure 1

A case with no-flow boundary

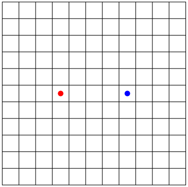

- pressure 0
- pressure 1

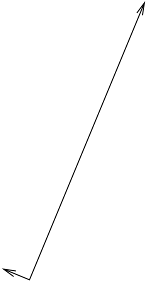

Anisotropy 1:1000
Angle 67.5 °

A case with no-flow boundary

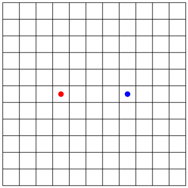

- pressure 0
- pressure 1

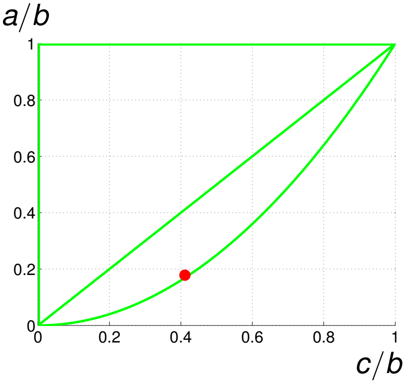

$a/b = 0.41$
$c/b = 0.17$

11×11 grid

11×11 grid

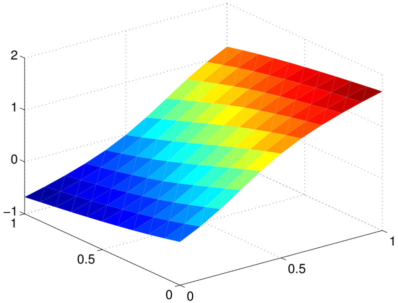

L-method

11×11 grid

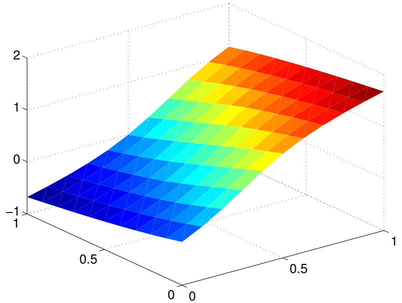

L-method

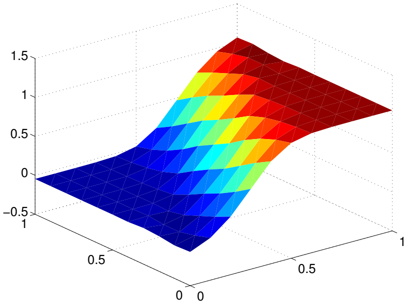

O(0)-method

11 × 11 grid

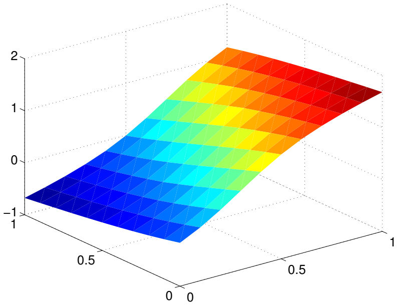

L-method

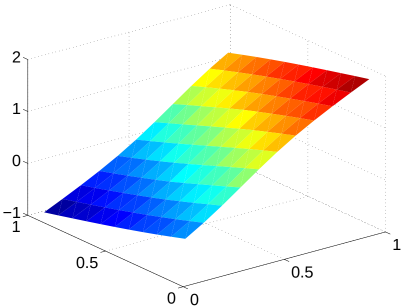

E1-method

11×11 grid

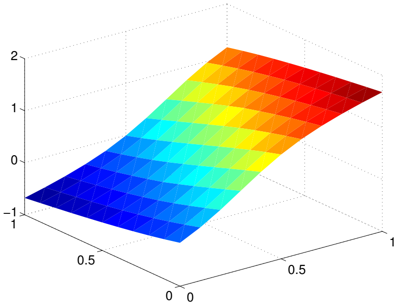

L-method

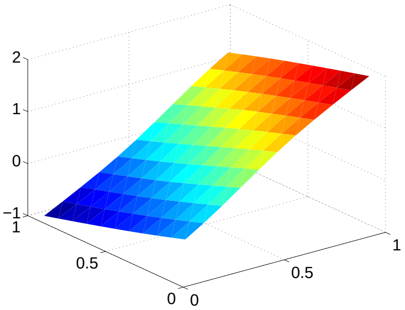

E2-method

55×55 grid

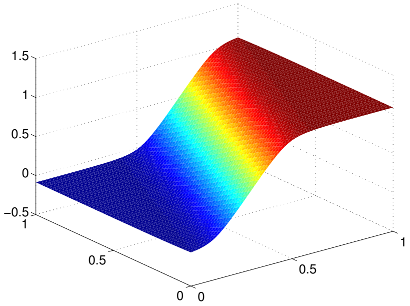

L-method O(0)-method

11 × 11 grid, Angle 45°

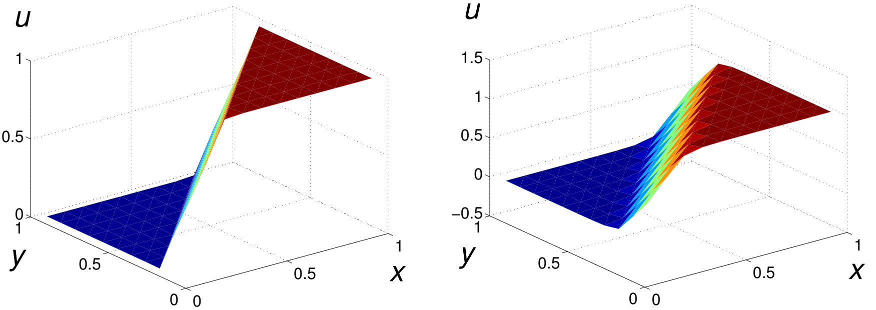

L-method O(0)-method

11×11 grid, source and sink

11×11 grid, source and sink

Extrema on no-flow boundary (violation of Hopf 2):

11×11 grid, source and sink

Extrema on no-flow boundary (violation of Hopf 2):

- O much better than L, E1 and E2,

11×11 grid, source and sink

Extrema on no-flow boundary (violation of Hopf 2):

- O much better than L, E1 and E2,
- L somewhat better than E1 and E2.

Outline

Test grids

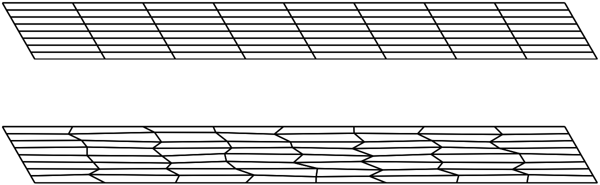

Test grids

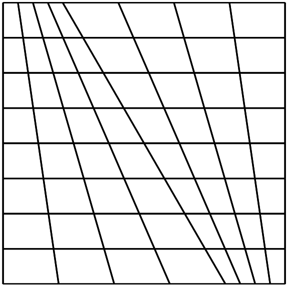

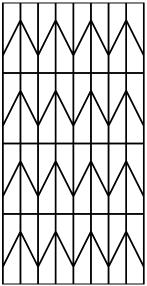

Test cases, streamlines

Smooth solution:

Nonsmooth solutions:

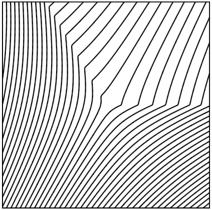

$u \in H^{2.29}$

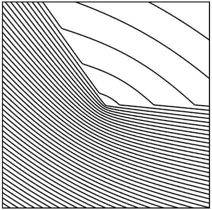

$u \in H^{1.79}$

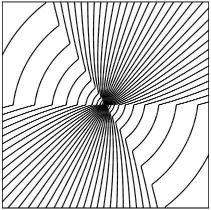

$u \in H^{1.24}$

Comparisons

Comparisons

Compare convergence behavior of L-, O(0)- and O(0.5)-method.

Comparisons

Compare convergence behavior of L-, O(0)- and O(0.5)-method.

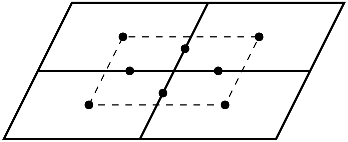

O(η)-method

Comparisons

Compare convergence behavior of L-, O(0)- and O(0.5)-method.

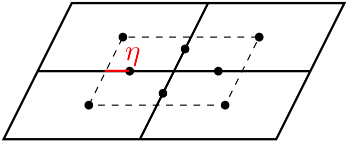

O(η)-method

Parallelogram grid, aspect ratio 1, angle 30 $^\circ$

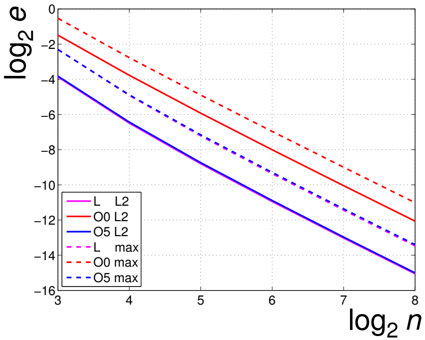

Pressure

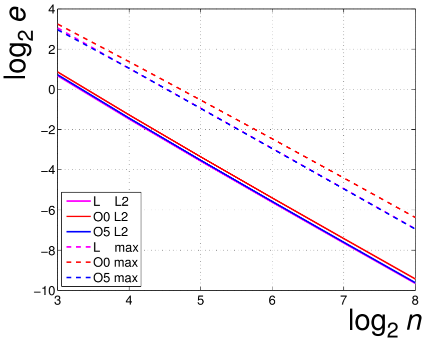

Normal flow density

Parallelogram grid, aspect ratio 0.01, angle 30 °

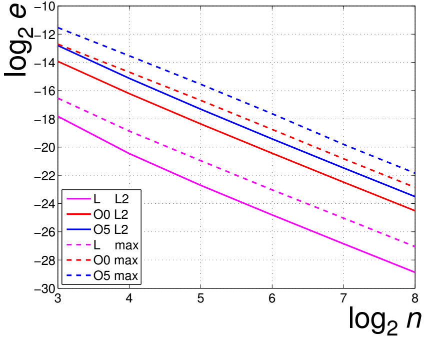

Pressure

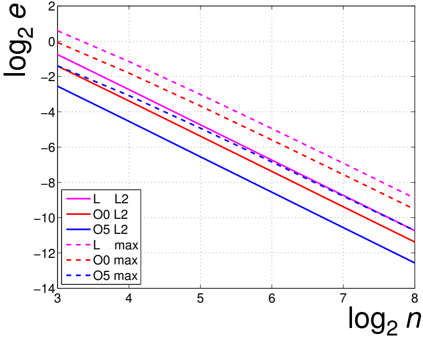

Normal flow density

Perturbed parallelogram grid, aspect ratio 0.1, angle 30 $^\circ$

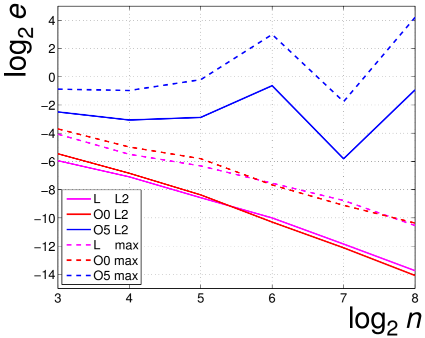

Pressure

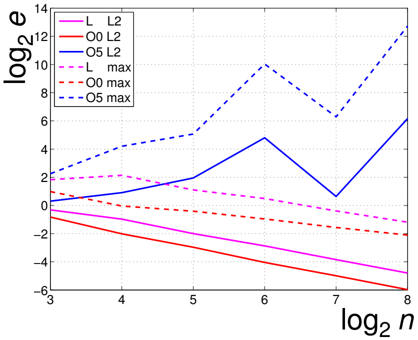

Normal flow density

Perturbed parallelogram grid, aspect ratio 0.01, angle 30 $^\circ$

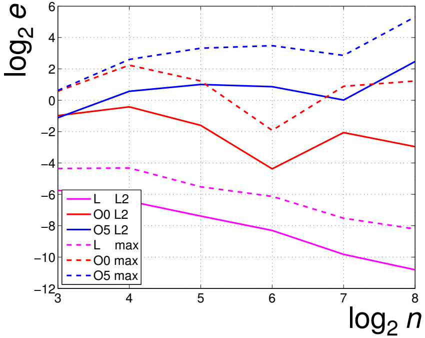

Pressure

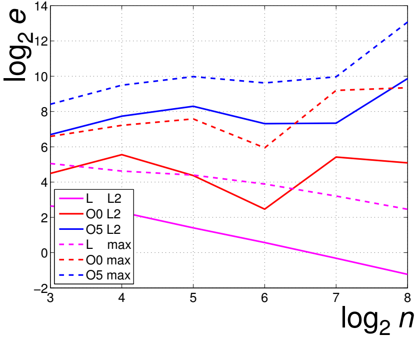

Normal flow density

Flow around a corner, $u \in H^{1.79}$

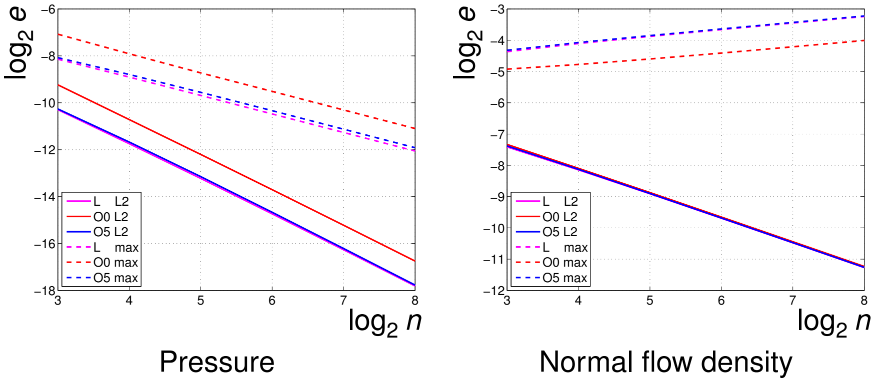

Convergence tests

Convergence tests

Tested L^2 and L^∞ convergence for

- solutions $u \in H^{1+\alpha}$, $\alpha > 0$,

Convergence tests

Tested L^2 and L^∞ convergence for

- solutions $u \in H^{1+\alpha}$, $\alpha > 0$,
- smooth and rough grids,

Convergence tests

Tested L^2 and L^∞ convergence for

- solutions $u \in H^{1+\alpha}$, $\alpha > 0$,
- smooth and rough grids,
- grid aspect ratios between 10^{-2} and 10^2,

Convergence

Convergence

On rough quadrilateral grids, the simulation tests indicate that if $u \in H^{1+\alpha}$, $\alpha > 0$, then

$$\|u_h - u\|_{L^2} \sim h^{\min\{2,2\alpha\}}$$

$$\|u_h - u\|_{L^\infty} \sim h^{\min\{2,\alpha\}}$$

$$\|(\boldsymbol{q}_h - \boldsymbol{q}) \cdot \boldsymbol{n}\|_{L^2} \sim h^{\min\{1,\alpha\}}$$

Convergence

On rough quadrilateral grids, the simulation tests indicate that if $u \in H^{1+\alpha}$, $\alpha > 0$, then

$$\|u_h - u\|_{L^2} \sim h^{\min\{2,2\alpha\}}$$

$$\|u_h - u\|_{L^\infty} \sim h^{\min\{2,\alpha\}}$$

$$\|(\boldsymbol{q}_h - \boldsymbol{q}) \cdot \boldsymbol{n}\|_{L^2} \sim h^{\min\{1,\alpha\}}$$

On smooth quadrilateral grids, stronger flow density bounds apply:

$$\|(\boldsymbol{q}_h - \boldsymbol{q}) \cdot \boldsymbol{n}\|_{L^2} \sim h^{\min\{2,\alpha\}}$$

$$\|(\boldsymbol{q}_h - \boldsymbol{q}) \cdot \boldsymbol{n}\|_{L^\infty} \sim h^{\min\{2,\alpha-1\}}$$

Convergence

On rough quadrilateral grids, the simulation tests indicate that if $u \in H^{1+\alpha}$, $\alpha > 0$, then

$$\|u_h - u\|_{L^2} \sim h^{\min\{2,2\alpha\}}$$
$$\|u_h - u\|_{L^\infty} \sim h^{\min\{2,\alpha\}}$$
$$\|(\boldsymbol{q}_h - \boldsymbol{q}) \cdot \boldsymbol{n}\|_{L^2} \sim h^{\min\{1,\alpha\}}$$

On smooth quadrilateral grids, stronger flow density bounds apply:

$$\|(\boldsymbol{q}_h - \boldsymbol{q}) \cdot \boldsymbol{n}\|_{L^2} \sim h^{\min\{2,\alpha\}}$$
$$\|(\boldsymbol{q}_h - \boldsymbol{q}) \cdot \boldsymbol{n}\|_{L^\infty} \sim h^{\min\{2,\alpha-1\}}$$

These rates apply to “moderate” aspect ratios.

Local grid refinement

Local grid refinement

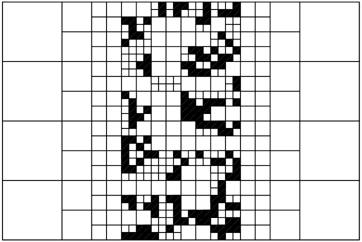

Black cells: $\boldsymbol{K} = 10^{-6}\boldsymbol{I}$. White cells: $\boldsymbol{K} = \boldsymbol{I}$.

Local grid refinement

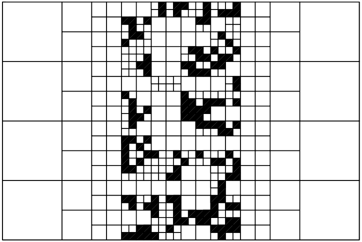

Black cells: $\boldsymbol{K} = 10^{-6}\boldsymbol{I}$. White cells: $\boldsymbol{K} = \boldsymbol{I}$.

- L-method error $\approx$ Fine-grid error.

Local grid refinement

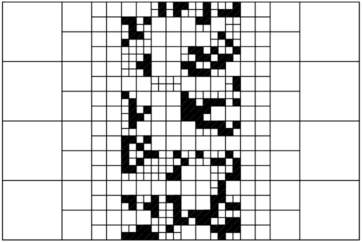

Black cells: $\boldsymbol{K} = 10^{-6}\boldsymbol{I}$. White cells: $\boldsymbol{K} = \boldsymbol{I}$.

- L-method error $\approx$ Fine-grid error.
- O-method error $\approx 2\times$ Fine-grid error.

Local grid refinement

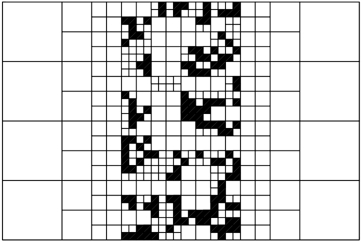

Black cells: $\boldsymbol{K} = 10^{-6}\boldsymbol{I}$. White cells: $\boldsymbol{K} = \boldsymbol{I}$.

- L-method error $\approx$ Fine-grid error.
- O-method error $\approx 2\times$ Fine-grid error.
- $\Rightarrow$ L-method almost optimal.

Outline

3D stencil, O-method

3D stencil, O-method

In 3 dimensions, the interaction volume contains 8 cells. For the O-method, the flux stencil has 18 cells, and the cell stencil has 27 cells.

3D stencil, O-method

In 3 dimensions, the interaction volume contains 8 cells. For the O-method, the flux stencil has 18 cells, and the cell stencil has 27 cells.

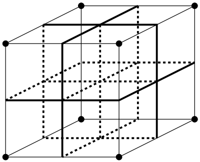

Interaction volume

3D stencil, O-method

In 3 dimensions, the interaction volume contains 8 cells. For the O-method, the flux stencil has 18 cells, and the cell stencil has 27 cells.

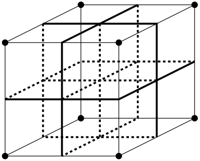

Interaction volume

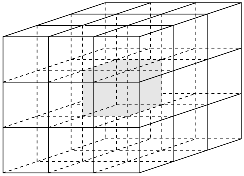

Cell stencil
O-method

3D L-stencils

3D L-stencils

In 3 dimensions there are 4 L-stencils with 4 cells.

3D L-stencils

In 3 dimensions there are 4 L-stencils with 4 cells.

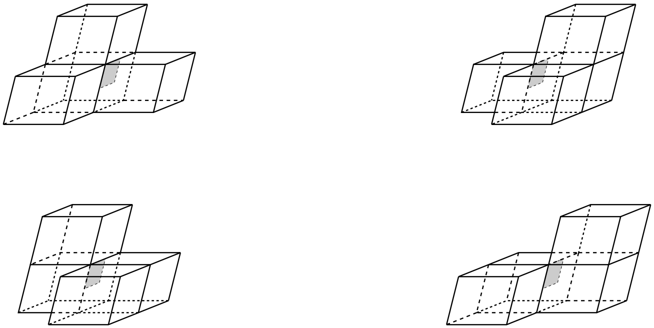

3D stencils, L-method

3D stencils, L-method

- Flux stencil: 10 points

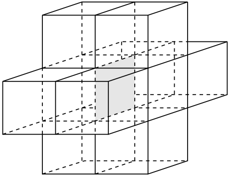

Flux stencil

3D stencils, L-method

- Flux stencil: 10 points
- Cell stencil: 19 points

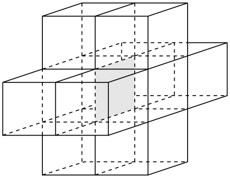

Flux stencil

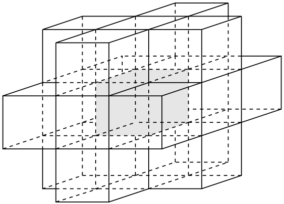

Cell stencil

3D flux stencils for constant “principal” directions, L-method

3D flux stencils for constant “principal” directions, L-method

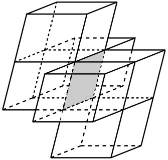

i direction

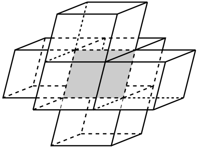

j direction

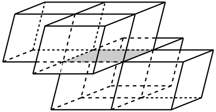

k direction

Cell stencil for constant "principal" directions, L-method

Cell stencil for constant “principal” directions, L-method

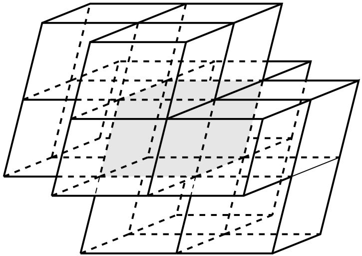

Cell stencil for constant “principal” directions, L-method

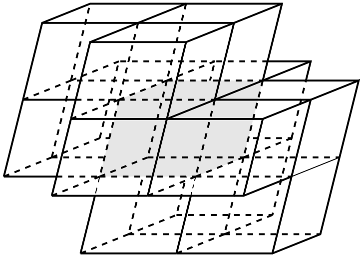

The cell stencil contains only 13 cells.

L-method, hanging node

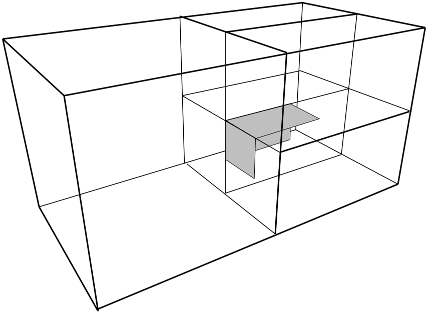

L-method, hanging node

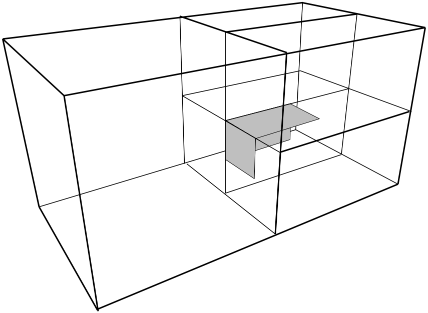

- Degrees of freedom: $3 \cdot 4 = 12$

L-method, hanging node

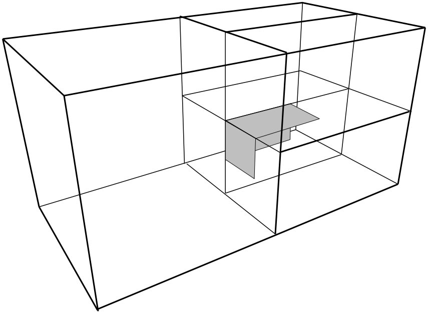

- Degrees of freedom: $3 \cdot 4 = 12$
- Continuity conditions: $4 \cdot 3 = 12$

Nonmatching grids

Nonmatching grids

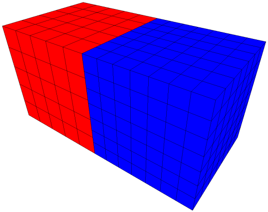

Nonmatching grids

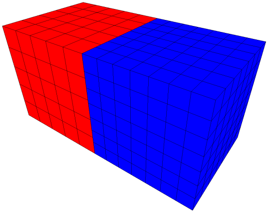

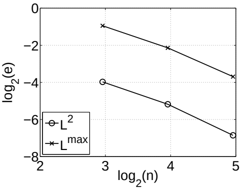

Pressure

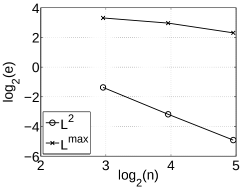

Normal flow density

Nonmatching grids

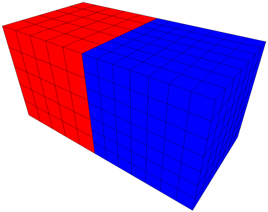

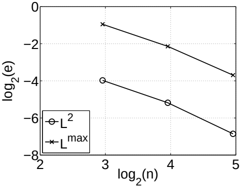

Pressure

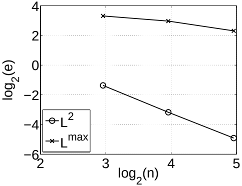

Normal flow density

L^2 convergence order: 1.7 for pressure and flow density

Two-phase flow

Two-phase flow

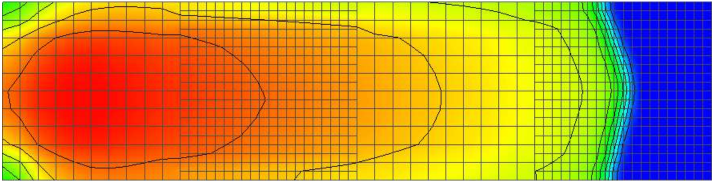

Saturation contours

Summary

Summary

- MPFA methods are well suited for reservoir simulation on quadrilateral grids.

Summary

- MPFA methods are well suited for reservoir simulation on quadrilateral grids.
- Good convergence and monotonicity properties can be shown for chosen stencils.

Summary

- MPFA methods are well suited for reservoir simulation on quadrilateral grids.
- Good convergence and monotonicity properties can be shown for chosen stencils.
- The solutions are exact for linear pressure fields.

Summary

- MPFA methods are well suited for reservoir simulation on quadrilateral grids.
- Good convergence and monotonicity properties can be shown for chosen stencils.
- The solutions are exact for linear pressure fields.
- Monotonicity conditions are generally more restrictive than L^2 convergence conditions.

Summary

- MPFA methods are well suited for reservoir simulation on quadrilateral grids.
- Good convergence and monotonicity properties can be shown for chosen stencils.
- The solutions are exact for linear pressure fields.
- Monotonicity conditions are generally more restrictive than L^2 convergence conditions.
- The L-method may also be used for nonmatching grids.

Recent papers

- I. Aavatsmark, G.T. Eigestad, R.A. Klausen, M.F. Wheeler, and I. Yotov, Convergence of a symmetric MPFA method on quadrilateral grids, *Comput. Geosci.* 11:333–345, 2007.
- R.A. Klausen and R. Winther, Robust convergence of multi point flux approximations on rough grids, *Numer. Math.* 104:317–337, 2006.
- J.M. Nordbotten, I. Aavatsmark, and G.T. Eigestad, Monotonicity of control volume methods, *Numer. Math.* 106:255–288, 2007.
- I. Aavatsmark, G.T. Eigestad, B.T. Mallison, and J.M. Nordbotten A compact multipoint flux approximation method with improved robustness, *Numer. Methods Partial Diff. Eqns.* 24, 2008.